This paper is available on line at http://www.mcponline.org

Global Impact of *Salmonella* Pathogenicity Island 2-secreted Effectors on the Host Phosphoproteome*[S]

Koshi Imami‡§, Amit P. Bhavsar¶‖, Hongbing Yu¶, Nat F. Brown, Lindsay D. Rogers‡ ‡‡, B. Brett Finlay¶‡‡§§, and Leonard J. Foster‡ ‡‡¶¶**

During the late stages of infection, *Salmonella* secretes numerous effectors through a type III secretion system that is encoded within *Salmonella* pathogenicity island 2 (SPI2). Despite the importance of SPI2 as a major virulence factor leading to the systemic spread of the bacteria and diseases, a global view of its effects on host responses is still lacking. Here, we measured global impacts of SPI2 effectors on the host phosphorylation and protein expression levels in RAW264.7 and in HeLa cells, as macrophage and nonphagocytic models of infection. We observe that SPI2 effectors differentially modulate the host phosphoproteome and cellular processes (*e.g.* protein trafficking, cytoskeletal regulation, and immune signaling) in a host cell-dependent manner. Our unbiased approach reveals the involvement of many previously unrecognized proteins, including E3 ligases (HERC4, RanBP2, and RAD18), kinases (CDK, SIK3, and WNK1), and histones (H2B1F, H4, and H15), in late stages of *Salmonella* infection. Furthermore, from this phosphoproteome analysis and other quantitative screens, we identified HSP27 as a direct *in vitro* and *in vivo* molecular target of the only type III secreted kinase, SteC. Using biochemical and cell biological assays, we demonstrate that SteC phosphorylates multiple sites in HSP27 and induces actin rearrangement through this protein. Together, these results provide a broader landscape of host players contributing to specific processes/pathways mediated by SPI2 effectors than was previously appreciated. ***Molecular & Cellular Proteomics 12: 10.1074/mcp.M112.026161, 1632–1643, 2013.***

Type III secretion systems (T3SSs)[1] are specialized virulence factors in Gram-negative pathogens that play an important role in delivering effector proteins to host cells. *Salmonella enterica* employs two distinct T3SSs encoded in *Salmonella* pathogenicity islands 1 and 2 (SPI1 and SPI2), with numerous effectors encoded around the genome, including a small number in SPI1 and SPI2 (1). SPI1 T3SS effectors are required for the bacterial internalization by intestinal epithelial cells at early stages of infection after oral ingestion. Although *Salmonella* is subsequently taken up by intestinal macrophages via phagocytosis, SPI2 T3SS effectors function to promote intracellular replication. Part of the role of SPI2 effectors is to control the maturation of the membrane-enclosed, *Salmonella*-containing vacuole (SCV) where *Salmonella* survives and replicates, eventually leading to a systemic infection known as typhoid fever (2, 3).

Approximately 30 effectors are known to be translocated by the SPI2 T3SS but the actions and targets of most of these effectors are largely unknown (1, 3, 4). A recent systematic study using a single mutant collection of SPI2 genes showed particular virulence factors (*e.g.* SpvB, SifA, and SteC) play a dominant role in replication within macrophages (5). It is known that SpvB induces cytotoxicity through its ADP-ribosyltransferase activity (6), and SifA is required for maturation of the SCV and the formation of *Salmonella*-induced filaments (7). SteC has been identified as the sole serine/threonine protein kinase encoded in the *Salmonella* genome (8), but the target substrates of this kinase within the host are not fully understood, although it has been demonstrated that SteC partially targets the MAP kinase MEK (9). Interestingly, SteC is capable of promoting assembly of an F-actin meshwork around the SCV; this is dependent on its kinase activity but does not require activation of signaling pathways through Rho-associated protein kinase (8), Cdc42, Rac, N-WASP, Scar/WAVE, and Arp2/3 (10). These host signaling proteins are the main targets of T3SS-secreted effectors from many pathogens, including the SPI1 system in *Salmonella* (11) and *Shigella* (12). Therefore, SteC is thought to manipulate

From the ‡Centre for High-Throughput Biology, ¶Michael Smith Laboratories, and Departments of ‡‡Biochemistry and Molecular Biology and §§Microbiology and Immunology, University of British Columbia, Vancouver, British Columbia V6T 1Z4, Canada and the **Department of Microbiology and Immunology, University of Melbourne, Victoria 3010, Australia

Received November 27, 2012, and in revised form, February 21, 2013

Published, MCP Papers in Press, March 3, 2013, DOI 10.1074/mcp.M112.026161

[1] The abbreviations used are: T3SS, type III secretion system; SPI, *Salmonella* pathogenicity island; SCV, *Salmonella*-containing vacuole; SILAC, stable isotope labeling by amino acids in cell culture; GO, gene ontology; IP-MS, immunoprecipitation-mass spectrometry; KEGG, Kyoto Encyclopedia of Genes and Genomes; PTM, Post-translational modification.

actin in a unique way through phosphorylation of host protein target(s).

Recent advances in high throughput measurements allow us to characterize host gene expression profiles (13) and host phosphoproteme dynamics (14) dependent on the presence of SPI1 effectors in an unbiased, comprehensive manner. However, although it is clear that SPI2 T3SS is a major virulence factor contributing to systemic infection, our knowledge of its effects on host responses is limited. In this study, we used a mass spectrometry (MS)-based quantitative proteomics approach and measured global host phosphorylation changes as well as proteome abundance altered by SPI2 effectors. Furthermore, we explore a molecular target of SPI2 effector kinase SteC by integrating the phosphoproteomics data and other quantitative proteomics screens.

EXPERIMENTAL PROCEDURES

Cloning and Purification of steC—The *steC* open reading frame was PCR-amplified from *Salmonella typhimurium* SL1344 genomic DNA to include XhoI and NotI restriction sites for cloning purposes. The fragment was cloned into pGEX(3HA) using the same restriction site as indicated in Ref. 15. Expression and purification of recombinant GST-3×HA-SteC were performed as in Ref. 15. For expression of *steC* in HeLa, the *steC* region from the pGEX(3HA) vector was ligated into a pcDNA3(2HA) expression vector using NotI and EcoRI enzymes.

SILAC Labeling and Salmonella Infection—RAW264.7 and HeLa cells (American Type Culture Collection) were cultured and labeled in arginine- and lysine-free Dulbecco's modified Eagle's medium (DMEM) (Caisson Laboratories Inc.) containing 10% (v/v) dialyzed fetal bovine serum (Invitrogen) in the presence of either L-arginine and L-lysine ("light" form) or L-[$^{13}C_6$,$^{15}N_4$]arginine and L-[$^{13}C_6$,$^{15}N_2$]lysine ("heavy" form). *Salmonella* (WT SL1344, SL1344Δ*ssaR,* or SL1344Δ*steC*) infection was done at a multiplicity of infection of 100 for 8 h as described previously (5). After the infection, cells were washed with ice-cold phosphate-buffered saline (PBS), harvested on ice, and frozen at −80°C until use. For the replication assay, one-tenth of the collected cells from a 10-cm culture dish was used, and bacteria were released from host cells using lysis buffer containing 1% Triton X-100 and 0.1% SDS in PBS. Recovered bacteria were plated in a dilution series, and the number of colony-forming units (CFU) was determined. All experiments using human cell lines were conducted according to institutional regulations.

SILAC Immunoprecipitation—For transfection of 2×HA-SteC, HeLa cells were seeded in SILAC medium (light) at a density of 4E+06 cells/dish in a 15-cm dish and transfected the following day with 20 μg/dish FuGENE (Promega)-complexed DNA. Cell lysates were harvested 24 h after transfection. Heavily labeled HeLa cells were mixed with the transfected cells (light). Cell lysis, immunoprecipitation, and subsequent LC-MS/MS analysis were performed as described previously (15) except that Magnosphere™ MS300/carboxyl (JSR Corp.) conjugated with mouse-α-HA (clone 2C16) (Santa Cruz Biotechnology) was used for immunoprecipitation.

Sample Preparation—Pellets of light and heavy labeled cells were combined, and cell lysis was performed as described elsewhere (16). Briefly, the cells were lysed with 50 mM ammonium bicarbonate and 1% (w/v) sodium deoxycholate, and each sample was boiled for 5 min. After protein reduction with dithiothreitol (DTT) and alkylation with iodoacetamide, trypsin digestion was performed overnight at 37°C. For phosphoproteome analyses, phosphopeptides were enriched using lactic acid-modified titanium dioxide (GL Sciences), followed by successive elution by 100 mM Na_2HPO_4, 5% (v/v) ammonium hydroxide, and 5% (v/v) pyrrolidine (17). For whole proteome analyses, peptides were fractionated to four fractions by C18-SCX-C18 StageTips (18). All resultant peptides were desalted using C18 StageTips (18) prior to LC-MS/MS analyses.

NanoLC-MS/MS Analysis—NanoLC-MS/MS analysis was conducted using an LTQ-Orbitrap Velos or XL mass spectrometer (Thermo Fisher Scientific) equipped with an 1100 series nanoflow HPLC system (Agilent) as described previously (14). An in-house analytical column (200-mm length × 75-μm inner diameter) was prepared with ReproSil-Pur C18-AQ materials (3 μm, Dr. Maisch). Settings for MS analysis are as follows: one full scan (resolution 60,000; *m/z* 300–1,600) followed by top 10 MS/MS scans using CID in the linear ion trap (minimum signal required, 200; isolation width, 3; normalized collision energy, 35; activation Q, 0.25; activation time, 10 ms) using dynamic exclusion (repeat count, 1; repeat duration, 30 s; exclusion list size, 500; exclusion duration, 60 s).

Data Analysis—For data analysis using MSQuant version 2.0a81 (19), peak lists were generated by Proteome Discoverer version 1.2 (Thermo Fisher Scientific) and searched against UniProt/Swiss-Prot (11/7/2011, subset human) plus SteC protein (total 20239 protein entries) using Mascot (version 2.1, Matrix Science). Search parameters included two missed cleavage sites, cysteine carbamidylmethyl-fixed modification, and variable modifications, including methionine oxidation, protein N-terminal acetylation, L-[$^{13}C_6$,$^{15}N_4$]arginine, L-[$^{13}C_6$,$^{15}N_2$]lysine, as well as phosphorylation of serine, threonine, and tyrosine. The peptide mass tolerance was 5 ppm and the MS/MS tolerance was 0.6 Da, and only peptides with Mascot scores ≥25 were considered. For raw data files obtained from the quantitative phosphoproteomics screen for discovery of substrates of SteC (see Fig. 4*B*), phosphopeptides showing significant increases upon SteC transfection were manually validated using MSQuant. All other data were analyzed and processed by MaxQuant (version 1.2.2.4) (20) using the same search parameters described above. The peptide mass tolerance was 6 ppm and the MS/MS tolerance was 0.5 Da. Database search was performed by means of Andromeda (21) against UniProt/Swiss-Prot (11/7/2011) *S. typhimurium* plus human (total 22,072 protein entries) or *S. typhimurium* plus mouse (total 18216 protein entries) with common serum contaminants and enzyme sequences. False discovery rate was set to 1% at peptide and at protein levels. Phosphorylation localization probabilities were defined as class I (localization probability, $p > 0.75$), class II ($0.75 > p > 0.5$), and class III ($p < 0.5$) based on PTM scoring (22). All quantified protein and peptide information can be found in the supplemental Tables 1–4. GO enrichment analysis was performed with the DAVID Functional Annotation Tool (23). Phosphorylation sequence motifs were searched with Motif-X (24). Kinase enrichment analysis was done using a web-based application tool (25).

In Vitro Kinase Assay—For the *in vitro* kinase assay, 0.1 μg of recombinant GST-3×HA-SteC was incubated with 1 μg of bovine myelin basic protein (Sigma) or 1 μg of human HSP27 (Abnova) in 25 μl of a reaction buffer containing 40 mM Tris-HCl, pH 7.5, 10 mM $MgCl_2$, 10 mM NaCl, 1 mM DTT, and 1 mM ATP, except that 0.1 mM ATP and 5 μCi of [γ-^{32}P]ATP were used for autoradiography. Incubation time was set for 30 min at 30°C for autoradiography and for 3 h at 37°C for LC-MS/MS analysis. For autoradiography, the protein mixture was subjected to SDS-PAGE and transferred to an Immun-Blot™ polyvinylidene fluoride (PVDF) membrane (Bio-Rad). For mass spectrometry analysis, the protein mixture was digested with trypsin as described above, and the resultant peptides were identified and quantified based on peak area.

Generation of Stable Cell Line—Using *S. typhimurium* SL1344 genomic DNA as a template, Myc-tagged SteC was amplified by PCR with primers that incorporated an XhoI site plus a Kozak and Myc tag

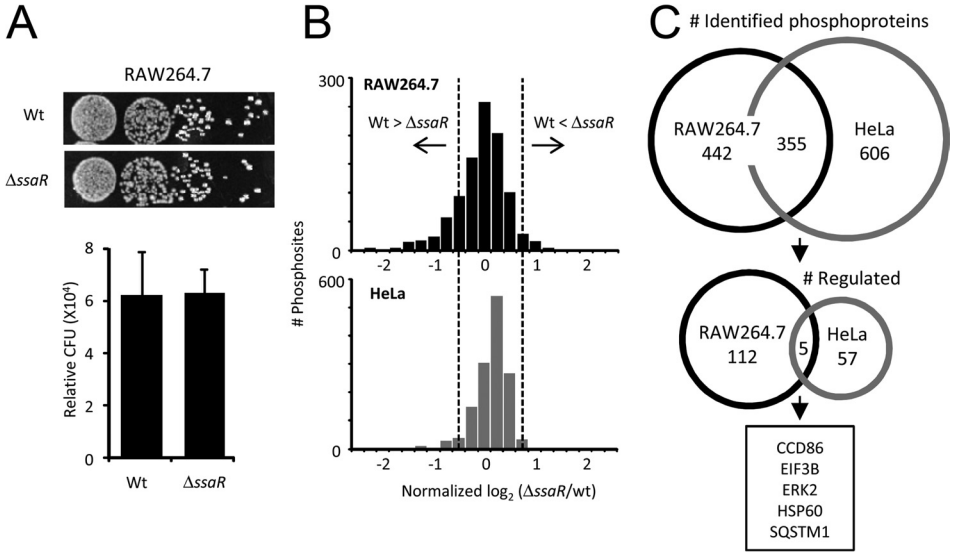

FIG. 1. **Overview of quantitative phosphoproteome profiling.** *A,* replication assay for WT and Δ*ssaR Salmonella* within light and heavy labeled RAW264.7, respectively, 8 h after infection. Recovered bacteria were plated in a dilution series, and the number of CFU (colony-forming units) was determined. The mean (±S.D.) count of relative CFU was determined from three independent experiments. *B,* histograms of $\log_2$-transformed SILAC ratios for all phosphosites quantified from RAW264.7 (*black*) and HeLa (*gray*). *Dashed lines* indicate the 95% confidence interval with no experimental perturbation. *C,* overlap of identified (*top*) and regulated (*bottom*) proteins between RAW264.7 and HeLa.

(underlined) sequence at the 5′ end (SteC-XhoI forward, 5′-GAA CTC TCG AGT TGC CAT GGA ACA GAA ACT CAT CTC AGA AGA GGA TCT GCC GTT TAC ATT TCA GAT CGG AAA TCA TAG T-3′) and an XbaI site at the 3′ end (SteC-XbaI reverse, 5′-GCA CGT CTA GAT TAT TTT TTT AAT TCA TCC TTT AAT ACC TTA GCC A-3′). The resulting PCR product was cloned into XhoI- and XbaI-digested lentivirus pLVX-puro vector (Clontech) to generate the lentiviral construct pLVX-puro-SteC. This construct was packaged into lentivirus particles in 293T cells (American Type Culture Collection) using lentiviral packaging mix (Sigma). HeLa cells were infected with these lentivirus particles and selected in culture media (DMEM) containing 3 μg/ml puromycin for 2 weeks. The stable cell line generated was designated as HeLa-Myc-SteC.

siRNA Knockdown and Drug Treatment—Myc-tagged SteC-expressing cells were seeded at 1.5×10^4 cells/well in a 24-well plate a day before transfection. Cells were transfected with INTERFERin (Polyplus transfection) for 48 h by following the manufacturer's protocol, and HSP27 siRNA UGA GAC UGC CGC CAA GUA A (target sequence) and control siRNA UAA GGC UAU GAA GAG AUA C (nontarget) (Dharmacon) were used at final concentration of 1 nM. Knockdown was confirmed by immunoblotting using rabbit α-HSP27 antibody (Abcam). For drug treatments using MEK inhibitors, stock solutions of 30 mM PD98059 (EMD Chemicals) and of 10 mM U0126 (EMD Chemicals) in dimethyl sulfoxide were diluted to a final concentration of 30 and 10 μM, respectively, with culture medium. Treatments were performed for 30 min at 37°C.

Immunofluorescence—Myc-tagged SteC-expressing cells were grown on 12-mm diameter glass coverslips. Cells were fixed with 2.5% paraformaldehyde solution made up in PBS with calcium and magnesium (+/+) for 15 min at RT, washed in PBS+/+, and blocked and permeabilized in 10% normal goat serum, 0.2% saponin for 10 min. Primary anti-Myc antibody (9E10, Developmental Studies Hybridoma Bank) was overlaid on coverslips for 30 min at RT at a dilution of 1:200 in the blocking/permeabilization solution. Cells were washed with PBS+/+, and a secondary Alexa Fluor 488 goat α-mouse IgG (Invitrogen) was overlaid on coverslips for 30 min at RT at a dilution of 1:500 in PBS+/+ with the blocking/permeabilization solution. Slides were mounted onto 1-mm glass slides using Prolong Gold antifade reagent (Invitrogen). Images were acquired on a Leica TCS SP5 II Confocal (Leica).

RESULTS

Quantitative Phosphoproteome and Proteome Profiling of the Host Cells Modulated by SPI2 Effectors—Intracellular replication of the SPI2 mutant (Δ*ssaR* (26)) strain was seen to decrease in macrophages (RAW264.7) more than 90% compared with the wild-type (WT) SL1344 strain (5). However, a functional SPI2 system is much less important when invading epithelial cells (HeLa and CaCo2) (5). Here, we used stable isotope labeling of amino acids in cell culture (SILAC) (27) coupled to liquid chromatography-tandem mass spectrometry (LC-MS/MS) and TiO_2 chromatography (28) to assess the impact of SPI2 T3SS on protein expression and phosphoprotein levels in two cell models of *Salmonella* infection (RAW264.7 and HeLa). *Salmonella* begins to express the SPI2 T3SS and effectors within a few hours after internalization into macrophages (29, 30), allowing the bacteria to start to replicate rapidly after 8 h (5). We chose to study this system 8 h post-infection because there are no discernable differences in intracellular bacteria between Δ*ssaR* and WT at this point (Fig. 1*A*) (5). Three thousand unique phosphopeptides from 797 proteins in RAW264.7 cells ($n = 3$, biological replicates) and 961 proteins in HeLa cells ($n = 2$) (false discovery rate <1%, at the peptide and at the protein level) were identified; only those phosphosites quantified in at least two biological replicates were used further (see supplemental Tables S1 and S2),

TABLE I

Impacts of Salmonella SPI2 effectors on protein phosphorylation, a list of selected proteins

Asterisk represents ambiguous phosphorylation sites.

Gene name	Protein name	RAW264.7		HeLa	
		Phospho site	Ratio (Δ*ssaR*/WT)	Phospho site	Ratio (Δ*ssaR*/WT)
Protein trafficking (total 19)					
Arap1	Arf-GAP with Rho-GAP domain	Ser-232*	0.47		
Rffl	E3 ubiquitin-protein ligase Raftlin	Ser-254	0.53		
Evl	Ena/VASP-like protein	Ser-327	0.55		
Msr1	Macrophage scavenger receptor types I and II	Ser-22*	0.56		
Sec22b	Vesicle-trafficking protein SEC22b	Ser-137	0.66		
Snap23	Synaptosome-associated protein 23	Ser-110	>10		
Immune signaling (total 13)					
Tyrobp	TYRO protein-tyrosine kinase-binding protein	Ser-90	0.40		
Marcksl1	MARCKS-related protein	Thr-14	0.44		
Mapk3	ERK1	Tyr-205	0.54		
Ship1	SHIP1	Ser-972	0.56		
Pak1	CDC42/RAC effector kinase PAK1	Thr-225	0.59		
Mapk1	ERK2	Tyr-185	0.61	Ser-190*	1.96
rkcd	PKCδ	Ser-643*	0.61		
Prkca	PKCα/β/γ			Thr-497	0.37
Cytoskeleton regulation (total 25)					
Cfl1	Cofilin1	Ser-3	0.47		
Dstn	Destrin (ADF)	Ser-3	0.51		
Stmn1	Stathmin	Ser-16	0.52		
Lsp1	Lymphocyte-specific protein 1	Thr-184*	0.59		
Slc9a1	Na^+/H^+ exchanger 1	Ser-801	0.62		
Hspb1	HSP27			Ser-15	0.19
Cdc42ep1	Cdc42 effector protein 1			Ser-121	0.40
Lima1	Eplin			Ser-726	0.52
Sptbn1	Spectrin β chain, brain 1			Ser-1447	0.55
Others					
Herc4	Probable E3 ubiquitin-protein ligase HERC4	Thr-329	0.21		
Znf828	Zinc finger protein 828	Ser-416	0.21		
Rftn1	Raftlin	Ser-243*	0.29		
Fcho2	FCH domain only protein 2	Thr-494*	0.30		
Sash1	SAM and SH3 domain-containing protein 1	Ser-83	0.32		
Eif3b	Eukaryotic translation initiation factor 3 subunit B	Ser-75*	0.54	Ser-154	0.06
Evi2b	Protein EVI2B	Ser-269,Ser-272	2.40		
Ppp1r2	Protein phosphatase inhibitor 2			Ser-122	0.06
Rune2	Protein prune homolog 2			Ser-595, Ser-597	0.23
Snd1	EBNA2 coactivator p100			Ser-426	0.30
Ttf1	Transcription termination factor 1			Ser-872	2.55

and of those, the relative standard deviation between replicates for 80% of these sites was less than 25%. A functional SPI2 system during infection had a much more dramatic effect on the phosphoproteome of macrophages than that of epithelial cells (Fig. 1*B*), so to explore the classes of proteins most impacted in the two different systems, we considered only those phosphorylation events that had a magnitude change of at least 1.5-fold, either up or down (which corresponds to the 95% confidence interval with no experimental perturbation, *dashed lines* in Fig. 1*B*) (Table I and supplemental Figs. S1 and S2). From the initial proteins, 117 (15% of total) met this criterion in RAW264.7 and 62 in HeLa cells (6% of total) (Fig. 1*C*), but despite a 40% overlap overall between the two phosphoproteomes, the regulated proteins in each cell type were nearly completely distinct (Fig. 1*C*). Of the few that were common to both, most are recognized as being central players in multiple diverse processes (*e.g.* ERK2, HSP60, SQSTM1, and EIF3B).

After an 8-h infection, observed changes in the phosphoproteome could be due to changes in the fraction of a protein that is phosphorylated but also to changes in protein expression (31); thus, we simultaneously measured the effect at 8 h after WT or Δ*ssaR* infections on overall changes in protein expression (supplemental Tables S3 and S4). The changes in expression as a result of a functional SPI2 system did not significantly affect the proteome profiles in either cell type (supplemental Fig. S1*A*); using the same criterion described above for determining whether a protein's expression was

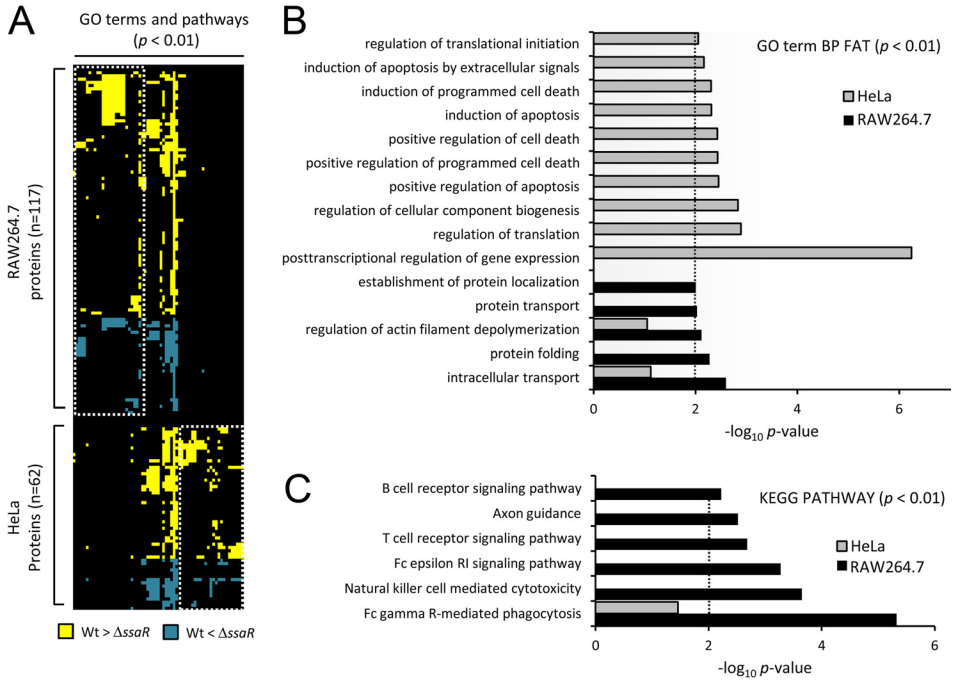

FIG. 2. **Host cell-specific modulation of cellular processes and pathways.** *A,* heatmap of the GO terms and KEGG pathways enriched ($p < 0.01$, *columns*) among the host proteins showing significant phosphorylation changes (*rows*). Gene enrichment analysis was done using DAVID (23). Where an intersection point is *colored*, it indicates that that term or pathway is assigned to the particular protein. *Yellow* or *blue* represents increased phosphorylation in WT *Salmonella* or in Δ*ssaR Salmonella*, respectively. *White dashed boxes* demark terms and pathways specific to either RAW264.7 or HeLa. *B* and *C,* plots of the $\log_{10}$ (*p* values) for some of the most highly enriched GO terms and KEGG pathways that correspond to columns in *A* (representative terms, *i.e.* GO term BP FAT and KEGG pathway, were shown, and results for all terms and pathways may be found in supplemental Fig. S2). The *dashed line* represents an arbitrary cutoff of $p < 0.01$).

regulated or not, only 4% of the proteome in each cell type was significantly changed (63 proteins in RAW264.7 and 61 proteins in HeLa). However, the possibility that changes in the levels of some specific proteins are the underlying reason for the apparent changes in phosphorylation cannot be completely ruled out as there is little overlap between phosphoproteome and proteome in our dataset. The majority of the regulated proteins both in RAW264.7 and HeLa cells were metabolic enzymes (supplemental Fig. S1*B*). The abundances of the classical phagosome or SCV marker proteins remained unchanged after 8 h of infection, including 10 Rab proteins, lysosomal glycoproteins (LAMP-1 and LAMP-2), V-ATPases (five subunits), cation-dependent mannose 6-phosphate receptor, and cathepsin D. The only exception to this was for transferrin receptor 1, an early SCV marker protein, which was reproducibly lower in WT-infected cells (Δ*ssaR*/WT = 1.60). Collectively, these results demonstrate that SPI2 effectors affect the two primary cell types targeted by *Salmonella* differently. Specifically, macrophages appear to be more broadly impacted than epithelial cells, consistent with a role for SPI2 T3SS as a main modulator for phagocytic cells (3–5).

Host Cell-specific Modulation of Phosphoproteome and Cellular Processes—To gain an unbiased picture of the processes targeted by the SPI2 system in epithelial cells and macrophages, we asked what cellular functions and pathways were enriched among the regulated phosphoproteins from each cell type, as defined by GO and Kyoto Encyclopedia of Genes and Genomes (KEGG; pathway categories) (23). An overview of enriched GO terms and pathways ($p < 0.01$) along with the host proteins showing significant phosphorylation changes is illustrated in Fig. 2*A*. Classes of proteins involved in "protein transport," "regulation of actin," and "immune signaling" were most impacted by SPI2 in RAW264.7 (Fig. 2, *B* and *C*; Table I). These results agree with previous findings where the main functions of SPI2 T3SS are thought to promote intracellular replication inside macrophages by altering host vesicular trafficking, cytoskeleton, and immune signaling (3, 4). Furthermore, these findings suggest that these cellular processes/pathways in RAW264.7 cells are principally regulated by SPI2 effectors at the phosphoproteome level. However, "apoptosis" and "regulation of gene expression" were most affected in HeLa cells (Fig. 2*B*), in agreement with previous reports that *Salmonella* does not induce rapid cell death in epithelial cells (32) but manipulates apoptosis using SPI2 effectors during late stage (at least 6 h) of infection (33, 34).

One of the main events during *Salmonella* infection is maturation of the SCV (7), concomitant with the manipulation of host phagosomal functions (35). Thirteen RAW264.7 proteins that play critical roles in these tracking events appear to be targeted for altered phosphorylation by the SPI2 system, including vesicle-trafficking protein SEC22b, synaptosome-as-

sociated protein 23 (SNAP23), and Ena/VASP-like protein (supplemental Fig. S3; Table I). SNAP23 phosphorylation regulates vesicular trafficking (*e.g.* membrane fusion and SNARE complex assembly) (36) so the down-regulation of SNAP23 phosphorylation at Ser-110 in WT-infected RAW264.7 cells (Δ*ssaR*/WT >10) suggests that SPI2 effectors may control vesicle trafficking between lysosome and SCV through dephosphorylation of SNAP23. Several hours post-infection, the SPI2 effector SteC and presumably other SPI2 effectors (SspH2, SpvB, and SrfH) are thought to modify the interactions between host actin and the SCV (37). Although it is known that destrin actin depolymerizing factor (ADF)/cofilin1 and Cdc42 effector 1, found to be modulated in this study, are controlled by pathogens through phosphorylation (38), we characterized additional cytoskeletal regulators (*e.g.* HSP27, stathmin, eplin, and spectrin β chain, brain 1) as well as their phosphorylation sites that would contribute to actin polymerization/depolymerization (39) for cytoskeletal reorganization. Importantly, many previously unrecognized proteins that potentially function during late stages of the infection were identified, including E3 ligases (HERC4 and RAD18) and Raftlin and histones (H2BF1, H4, and H15) (supplemental Fig. S3; Table I). HERC4 (40) was reported to involve protein trafficking, whereas RAD18 appears to be required for DNA repair (41). Raftlin is important for formation and/or maintenance of lipid rafts and regulates B-cell antigen receptor-mediated signaling (42). Overall, the unbiased approach to understand the role of SPI2 in infection identified several components of key cellular processes (*e.g.* protein trafficking, cytoskeletal regulation, immune signaling, and apoptosis) that help to rationalize observations about *Salmonella* pathogenesis; we also identified several host proteins regulated by *Salmonella* that do not fit into our current models of the infection process (supplemental Fig. S3; Table I), suggesting that there is much more to be learned.

Kinases Modulated by SPI2 Effectors—Changes in phosphorylation must be a result of altered kinase and/or phosphatase activity. Because phosphorylation plays a more important role in the acute regulation of kinases than of phosphatases, we next asked which host kinases are targeted by SPI2 effectors. A total of 61 kinases were detected in the phosphoproteome of macrophages, including AKT1, FAK1, and RAF1. Among those quantified in at least two biological replicates, the phosphorylation states of 10 (CDK1/2/3, ERK1/2, KAP0 (PKA), KPCD (PKCδ), PAK1 (STE20 homolog), SIK3, WNK1) were shown to be dependent on SPI2 effectors (Fig. 3*A*). As a means of predicting the kinases that might be responsible for the gross effects of SPI2-regulated phosphorylations, we performed a motif-based analysis (24) and sought consensus sequence motifs from the list of the regulated phosphopeptides containing class I phosphorylation sites. In RAW264.7, a classic proline-directed phosphorylation motif (-SP-) attributed to MAPK and CDK as well as the R*XX*S motif common to PKA, PKC, and CaMK2 were particularly enriched among those proteins whose phosphorylation was increased in WT-infected cells (Fig. 3*B*). Orthogonally to this, kinase enrichment analysis (25) showed that in our phosphoproteome data of RAW264.7 substrates, likely targets of nine kinase families, were enriched, including STE20, MAPK, PKC, CDK, and PKA ($p < 0.05$) (Fig. 3*C*). Together, our experimental phosphoproteomic data and bioinformatic analyses consistently suggest that ERK1/2, CDK, PKA, and PKC are key regulators in the macrophages at the late stage of infection.

PKC, in particular, could be a master regulator throughout *Salmonella* infection as an inhibitor of PKC significantly decreased IL-8 secretion during SPI1 effector-mediated infections (14). In our current data, phosphorylations of Ser-643 of PKCδ in RAW264.7 and of Thr-497 of PKCα/β/ρ in HeLa cells are both up-regulated by about 2-fold by WT *Salmonella* (Fig. 3*A*; Table I), and both sites are required for full PKC activity (43). PKC plays an important role in apoptosis, cell cycle, immune response, and actin polymerization through directly or indirectly regulating downstream kinases CDK1 and

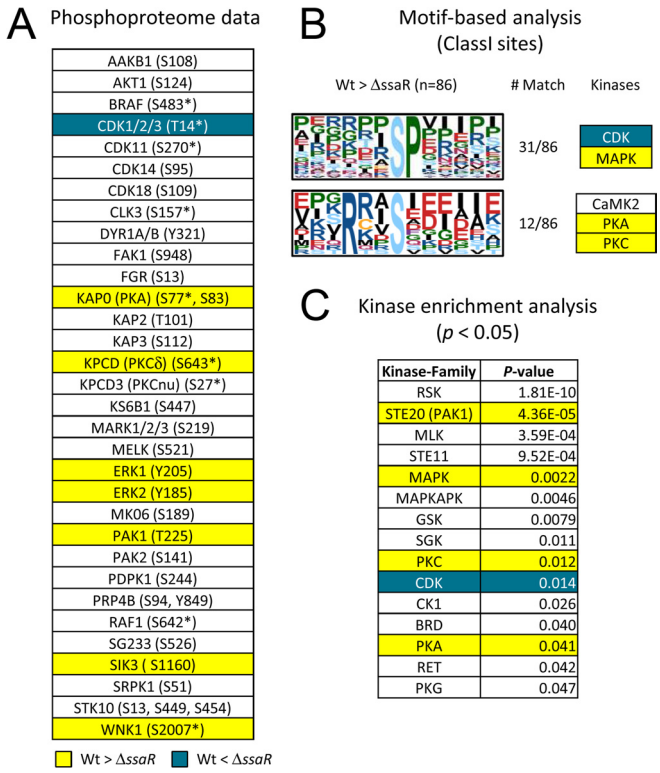

FIG. 3. **Protein kinase profiling in RAW264.7.** *A,* protein kinases quantified in this study. *Asterisks* represent ambiguous phosphorylation sites (*i.e.* class II or class III sites where the fragments detected are insufficient to assign the specific residue that is phosphorylated). *Yellow* and *blue* coloring indicates kinases that show phosphorylation increases in WT *Salmonella* and in Δ*ssaR Salmonella*, respectively. *B,* phosphorylation sequence motifs extracted from SPI2-regulated phosphosites by the Motif-X algorithm (24). *C,* protein kinase families enriched from SPI2-regulated phosphoproteins (substrates). These kinases were extracted based on a mammalian kinase-substrate database using kinase enrichment analysis tool (25).

ERK1/2 (44, 45). Indeed, CDK1/2/3 appear to be activated through dephosphorylation at Thr-14 or Tyr-15 (Δ*ssaR*/WT = 2.82), both of which inhibit kinase activity (Table I) (46). As for the ERK1/2, tyrosine phosphorylation at Tyr-205/Tyr-185 in ERK1/2 showed increased profiles (Δ*ssaR*/WT = 0.54 and Δ*ssaR*/WT = 0.61) in RAW264.7 cells, although in HeLa cells the threonine phosphorylation site at Thr-190 on ERK2 showed the opposite trend (Δ*ssaR*/WT = 1.96) (Table I). This observation is consistent with the fact that an SPI2 phosphothreonine lyase SpvC dephosphorylates the threonine sites in ERK1/2 (47) to inactivate them, subsequently inducing anti-inflammatory effect (48).

Identifying a Molecular Target of SPI2 Effector Kinase SteC—Bacteria have very few protein kinases compared with eukaryotes, but some pathogens have evolved to use their T3SSs to deliver kinase virulence factors to their host, *e.g.* YpkA of *Yersinia* inhibits GTP binding through phosphorylation of the host heterotrimeric G protein $G\alpha_q$ (49). Similarly, but with less mechanistic detail, a *Salmonella* SPI2 effector called SteC is known to manipulate actin using its kinase activity (8). As unbiased but indirect confirmation of this in this study, GO terms for "regulation of actin filament depolymerization," "actin binding," and "actin cytoskeleton" were enriched ($p < 0.01$), and phosphorylations of several actin-binding proteins were shown to increase by SPI2 effectors (Table I; supplemental Fig. S3).

To assess what host proteins might be direct targets of SteC, we employed phosphoproteomics technology in a different strategy than that used above, and we also tried to identify host binding partners of SteC by an immunoprecipitation-mass spectrometry (IP-MS) approach as we have done previously for most SPI effectors (15, 50). HeLa (light form) transfected with double hemagglutinin (2×HA)-tagged SteC and control HeLa (no transfection, heavy form) (Fig. 4*A*) were combined and analyzed by LC-MS/MS after either TiO_2 phosphoenrichment ($n = 2$) or IP with anti-HA antibody ($n = 1$). In the phosphoproteomics screen, we identified 15 actin-associated proteins (marked in *red* in Fig. 4*B, left*), including HSP27, eplin, and spectrin β chain, whose phosphorylation profiles were observed to be increased more than 2-fold upon SteC transfection. Note that some of these actin-binding proteins showed phosphorylation increases in the infection experiments as well (Table I and supplemental Fig. S3). For instance, phosphorylation of Ser-15 of HSP27 in particular was 5-fold higher in cells infected with WT *Salmonella versus* the Δ*ssaR* condition (Fig. 4*C, top*; Table I). In addition, we confirmed that Δ*steC Salmonella* cannot induce phosphorylation of Ser-15 (Fig. 4*C, bottom*). Furthermore, the IP-MS screen also identified HSP27 as a binding partner of SteC (ctrl/SteC-transfection = 0.27) (Fig. 4*D*), whereas the other actin-binding proteins did not show high specificity for SteC or were not detected. Thus, several lines of evidence point to host HSP27 as a likely direct target of SteC.

To verify whether SteC can directly phosphorylate HSP27, we performed an *in vitro* kinase assay using recombinant GST-3×HA-SteC and human HSP27. Activity of the recombinant SteC was first confirmed using myelin basic protein and autoradiography (Fig. 4*E*) as well as LC-MS/MS (supplemental Fig. S4). Recombinant HSP27 was then substituted as the phosphate receiver, and the reaction mixture was digested with trypsin prior to analysis with LC-MS/MS. In this artificial *in vitro* system, SteC was found to strongly phosphorylate at least six residues in HSP27 (Fig. 4*F, left panel*). Examples of extracted ion chromatograms of two phosphopeptides and a nonphosphorylated peptide from HSP27 are shown in Fig. 4*F, right panel,* and supplemental Fig. S5. The *in vivo* and *in vitro* data presented here confirm that SteC can directly phosphorylate HSP27 and that this possibly occurs *in vivo* as well, at least for Ser-15 of HSP27. These observations then suggest that SteC's effect on actin, known to be dependent on its kinase activity, is manifested through the regulation of HSP27 by phosphorylation.

Does SteC Manipulate Actin through HSP27?—We initially tried to observe the F-actin meshwork around SCV within WT-infected HeLa or NIH3T3 cells as reported before (8) but could not observe a similar phenotype. Since this could be due to our use of a different strain, we addressed the discrepancy by generating HeLa cells stably expressing Myc-tagged SteC and assessed if SteC can manipulate actin in the cells and if the phenotype could be influenced by knockdown of HSP27. In the SteC-expressing HeLa cells, actin became condensed as observed in Ref. 8, with only a few remaining filaments in 80% of the cells (Fig. 5*A*), although controls demonstrated normal actin filaments (supplemental Fig. S6). Next, we investigated if the actin condensation would disappear when HSP27 is knocked down by siRNA. The knockdown of HSP27 for 48 h (see Fig. 5*B*) resulted in a 50% decrease in the actin condensation (Fig. 5, *A* and *C*) compared with the control in which nontargeted siRNA was used (supplemental Fig. S6). The knockdown of HSP27 did not rescue the actin condensation completely, implying that the knockdown was not 100% and/or that other potential targets of SteC work in concert with HSP27. Recently Odendall *et al.* (9) reported that SteC targets the MEK pathway for actin cytoskeleton reorganization in NIH3T3 fibroblast cells. To assess whether the regulation of F-actin through HSP27 is independent of the MEK pathway, we further investigated actin structure of the SteC-expressing HeLa in the presence of a MEK inhibitor under the HSP27-knockdown condition. First, we treated the cells for 30 min with 30 μM PD98059, which was used in Ref. 9, or 10 μM U0126 (51), which is a more selective and more effective inhibitor than PD98059, but neither inhibitor diminished the actin condensation (Fig. 5, *A* and *C*, and supplemental Fig. S6). Thus, we could not observe the significant additional effect of the combination of the MEK inhibitors plus HSP27 siRNA compared with only HSP27 siRNA (Fig. 5, *A* and *C,* and supplemental Fig. S6).

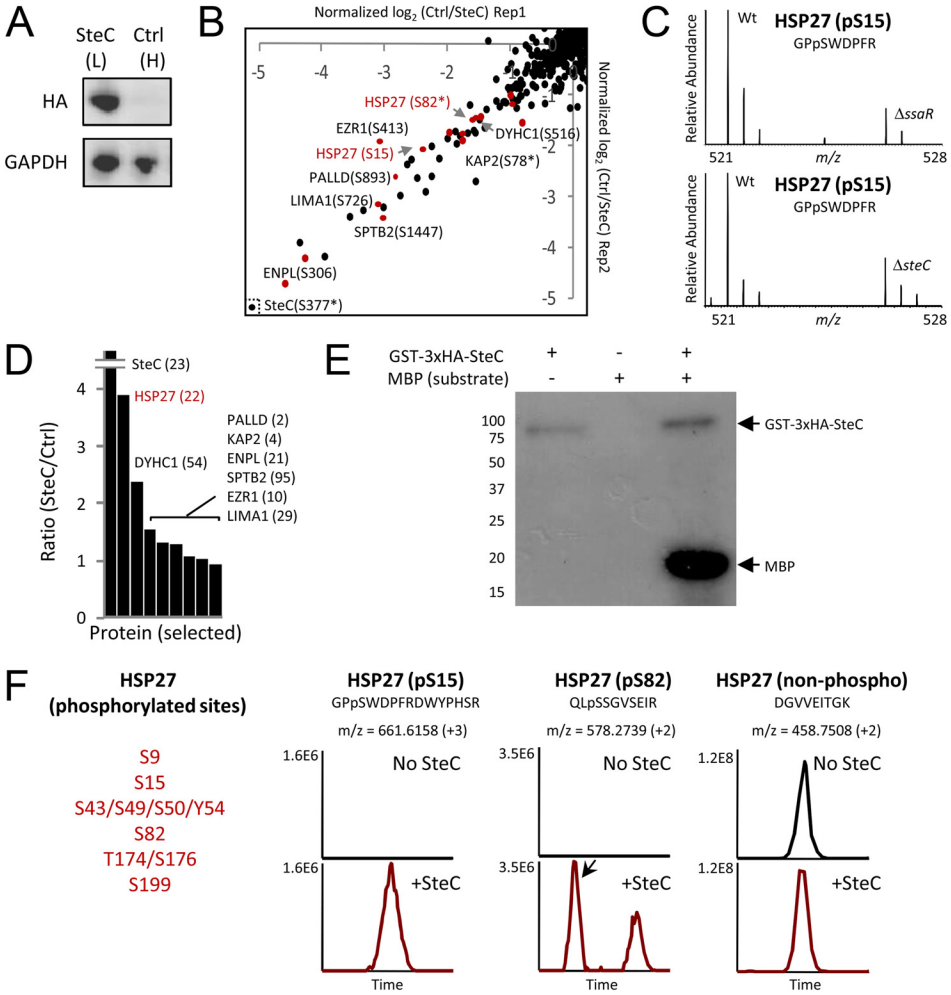

FIG. 4. **Quantitative screens to identify molecular targets of SteC.** *A,* HeLa cells (*L,* light form) were transfected with 2×HA-SteC, whereas no transfection was performed for control HeLa cells (*H,* heavy). Expressions of SteC and GAPDH (control) were confirmed by immunoblotting. *B,* phosphoproteomics screen for discovery of substrates. The *x* and *y* axis show relative phosphorylation changes (log_2-transformed H/L) of peptides upon SteC transfection in replicate 1 and in replicate 2, respectively. *Red dots* represent phosphopeptides from actin-associated proteins. *C,* phosphorylation change of HSP27 Ser-15 in infection experiments (8 h post-infection). WT *Salmonella* but not Δ*ssaR Salmonella* (*top panel*) and Δ*steC Salmonella* (**bottom panel**) induces HSP27 Ser-15 phosphorylation in HeLa. *D,* in the IP-MS screen for identifying binding partners of SteC, SteC-specific binding partners are identified by having an SteC/ctrl ratio significantly greater than 1. Only selected proteins (SteC and actin-associated proteins found in *B*) are shown, with the number of identified unique peptides in *parentheses*. *E* and *F, in vitro* kinase assay. *E,* GST-3×HA-SteC was incubated with a general kinase substrate myelin basic protein (MBP) and [γ-^{32}P]ATP. Proteins are separated by SDS-PAGE and detected by autoradiography. *F,* after an *in vitro* reaction of recombinant human HSP27 with or without GST-3×HA-SteC, proteins are subjected to tryptic digestion, followed by LC-MS/MS analysis. At least six sites in HSP27 were phosphorylated by the SteC based on extracted ion chromatograms of the identified peptides.

This means that the regulation of F-actin through HSP27 is independent of the MEK pathway and that SteC does not target MEK, at least in the HeLa cells. These results suggested that HSP27 is one of the, if not the primary, molecular targets of SteC and that it is capable of manipulating actin contributing to the formation of an F-actin meshwork in host cells.

DISCUSSION

Here, we provide the first analysis of the impact of SPI2 effectors on the host phosphoproteome and proteome using two common phagocytic and nonphagocytic host models of *Salmonella* infection. Although the majority of the molecular interactions between SPI2 effectors and host targets has yet to be defined and will be the subject of future investigations, in this study we have revealed a landscape of key host players and their phosphorylation sites involving particular cellular processes/pathways altered by SPI2 effectors (Fig. 2 and supplemental Fig. S3).

One striking observation from our study was the disparity in phosphoproteome profiles and cellular processes modulated by SPI2 in RAW264.7 and HeLa cells (Fig. 2 and

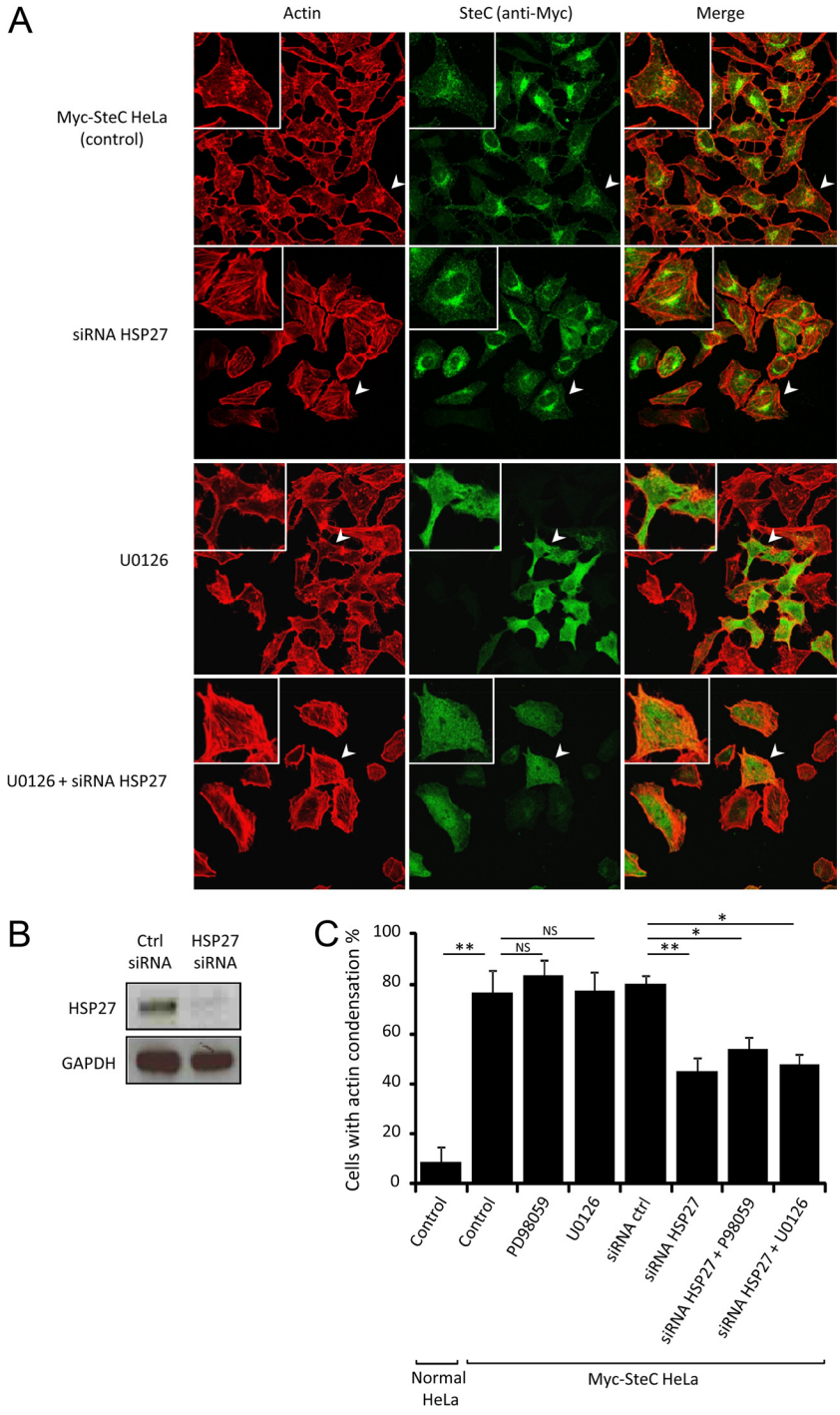

FIG. 5. **SteC manipulates actin through HSP27.** *A,* representative confocal images of HeLa cells stably expressing Myc-tagged SteC. Cells were immunolabeled with anti-Myc antibody (*green*), and F-actin was visualized by phalloidin conjugated to Alexa Fluor 568 (*red*). Cells were treated with siRNA (1 nM control siRNA and 1 nM HSP27 siRNA) and MEK inhibitors (30 μM PD98056 and 10 μM U0126). *B,* immunoblot analyses of Myc-tagged SteC HeLa in siRNA-transfected cell lysates. Immunoblots detected by anti-HSP27 antibody (*top panel*) and anti-GAPDH antibody (*control* (*Ctrl*), *bottom panel*) are shown to confirm knockdown of HSP27. *C,* quantification of cells with actin condensation. The means ($\pm$S.D.) of proportion of cells with actin condensation were determined from at least three independent experiments, in which a total of more than 100 cells were examined. Statistical analyses were performed with two-tailed unpaired Student's *t* test. *, $p < 0.001$; **, $p < 0.0001$.

supplemental Fig. S2). For example, SPI2 substrates modulated immune signaling and protein transport in RAW264.7 cells but modulated apoptosis in HeLa cells. It is tempting to speculate that SPI2 imparts a type of cell tropism, responding differently to macrophages *versus* epithelial cells, and how this might occur is an interesting question. One possibility is that SPI2 delivers a mixture of effectors into every cell type, but the targets of a given effector may be present or absent in that specific cell. More intriguing would be a scenario where a given SPI2 effector has different targets in distinct host cell types. Comparative studies between wild type and the SPI2 single deletion mutant library (5) in these types of global analyses might help to distinguish between these possibilities. Overall, the changes in the phosphoproteome mediated by the SPI2 T3SS were not nearly as dramatic as those we observed recently with SPI1 effectors at earlier infection times (14). There are several possible explanations for this as follows. 1) For the shorter incubations

in the previous study, we were able to remove serum from the culture media, something that was not possible in this study due to the longer incubation. This would have the effect of raising the base-line levels of phosphorylation significantly. 2) Because phosphorylation cascades usually occur within minutes and not hours, SPI2 effectors may simply have not evolved to use phosphorylation to achieve their effects to the extent that SPI1 effectors do (1). This is supported by the observation that SPI2 effectors seem to be required for long term intracellular processes to create a suitable replicative environment within host cells. 3) The longer infection time used here (24 times longer than previously) would allow plenty of time for the cells to lose synchronicity, effectively suppressing the effects of the infection when averaged across the population of cells. Indeed, it is difficult to accurately measure changes in phosphorylation such a long time after stimulation in any system; the only attempts we are aware of in *Salmonella* infection models targeted specific proteins, such as p38 (52) or members of the mTOR pathway (53). Obviously, there are still measurable changes occurring across a population though, and the SILAC approach used here allowed us to capture the changes in site-specific phosphorylation triggered by SPI2 T3SS in an unbiased, comprehensive manner.

As mentioned above, there are very few Ser/Thr kinases in bacteria, and an even smaller number of those are virulence factors. The key mechanistic contribution of the work presented here has been the demonstration that a secreted bacterial kinase can manipulate host actin remodeling through the direct phosphorylation of a single host protein. How this might occur at the atomic level is still an open question in the HSP27 field, although it seems likely that phosphorylation of HSP27 induces its disassociation from actin monomers, resulting in promotion of F-actin assembly from the newly freed actin monomers (54, 55). One prediction of this would then be that multiply phosphorylated forms of HSP27 could further accelerate actin polymerization. We present *in vitro* evidence that SteC is capable of phosphorylating at least six sites in HSP27 (Fig. 4*F* and supplemental Fig. S5), whereas one of HSP27's natural kinases in humans, MAPKAP2, can phosphorylate only three sites (Ser-15, Ser-78, and Ser-82) (56). This system differs from that used by *Listeria monocytogenes*, which manipulates the host p38 MAPK pathway to indirectly cause the phosphorylation of HSP27 to affect actin remodeling (54). More recently, two groups showed that SteC targets Cdc24 in yeast (57) and MEK in mammalian cells (9). We also identified MEK as a binding partner of SteC by the IP-MS screen (ctrl/SteC-transfection = 0.19) (data not shown) but could not detect any *in vitro* or *in vivo* phosphorylation of MEK by SteC. Because SteC could only be observed to phosphorylate MEK under forced conditions using purified versions of the two proteins, our data suggest that the stoichiometry of MEK phosphorylation *in vivo* may be relatively low. Despite this, the putative SteC phosphorylation site on MEK (Ser-200) does seem to play a role in actin rearrangement, although it cannot explain the whole effect because inhibition of MEK pathway only reduced F-actin meshwork by 50% (56). Importantly, our data suggest that MEK is unlikely to contribute to SteC-induced actin remodeling in HeLa cells (Fig. 5). A possible explanation for this is that there could be unique host targets of SteC in a cell type-specific manner, which is also supported by our phosphoproteomic data where we observed the disparity in phosphoproteome profiles modulated by SPI2 in the distinct cell types, as discussed above. In synthesis, our data in the context of these recent studies suggests that SteC-induced HSP27 phosphorylation is a parallel route to host actin manipulation and/or is cell type-specific. Further studies will be needed to fully understand the mechanism of the manipulation of actin through SteC-host protein interactions. The data presented here provide the missing link between SteC and actin manipulation, explaining how SteC's effects can be independent of the well known route to actin remodeling through Cdc42, Rac, N-WASP, Scar/WAVE, and Arp2/3, which are common targets of pathogens (10). Thus, the phosphorylation of HSP27 represents a novel mechanism for pathogen-induced manipulation of the actin cytoskeleton.

Acknowledgments—We thank Vincent Chen, Joost Gouw, Nikolay Stoynov, Joris van der Heijden, and Roland Scholz for helpful discussions; Qingning Zeng and Albert Cairo for assistance with the *in vitro* kinase assay; and Michelle Buckner for generously providing SL1344Δ*steC* strain.

* This work was supported in part by Canadian Institutes for Health Research Operating Grants MOP-10551 (to B.B.F.) and MOP-77688 (to L. J. F.).

S This article contains supplemental material.

§ Supported by a Japan Society for the Promotion of Science fellowship and a Government of Canada post-doctoral research fellowship.

‖ Present address: Dept. of Medical Genetics, The University of British Columbia.

¶¶ To whom correspondence should be addressed: Canada Research Chair in Quantitative Proteomics, 2125 East Mall, Vancouver, British Columbia V6T 1Z4, Canada. Tel.: 604-822-8311; E-mail: foster@chibi.ubc.ca.

REFERENCES

1. Haraga, A., Ohlson, M. B., and Miller, S. I. (2008) *Salmonella* interplay with host cells. *Nat. Rev. Microbiol.* **6,** 53–66
2. Abrahams, G. L., and Hensel, M. (2006) Manipulating cellular transport and immune responses: Dynamic interactions between intracellular *Salmonella enterica* and its host cells. *Cell. Microbiol.* **8,** 728–737
3. Garai, P., Marathe, S. A., and Chakravortty, D. (2011) Effectors of *Salmonella* pathogenicity island 2: An island crucial to the life of *Salmonella*. *Virulence* **2,** 177–180
4. Figueira, R., and Holden, D. W. (2012) Functions of the *Salmonella* pathogenicity island 2 (SPI-2) type III secretion system effectors. *Microbiology* **158,** 1147–1161
5. Buckner, M. M., Croxen, M. A., Arena, E. T., and Finlay, B. B. (2011) A comprehensive study of the contribution of *Salmonella enterica* serovar *typhimurium* SPI2 effectors to bacterial colonization, survival, and replication in typhoid fever, macrophage, and epithelial cell infection models. *Virulence* **2,** 208–216
6. Lesnick, M. L., Reiner, N. E., Fierer, J., and Guiney, D. G. (2001) The

Salmonella spvB virulence gene encodes an enzyme that ADP-ribosylates actin and destabilizes the cytoskeleton of eukaryotic cells. *Mol. Microbiol.* **39,** 1464–1470
7. Beuzón, C. R., Méresse, S., Unsworth, K. E., Ruíz-Albert, J., Garvis, S., Waterman, S. R., Ryder, T. A., Boucrot, E., and Holden, D. W. (2000) *Salmonella* maintains the integrity of its intracellular vacuole through the action of SifA. *EMBO J.* **19,** 3235–3249
8. Poh, J., Odendall, C., Spanos, A., Boyle, C., Liu, M., Freemont, P., and Holden, D. W. (2008) SteC is a *Salmonella* kinase required for SPI-2-dependent F-actin remodeling. *Cell. Microbiol.* **10,** 20–30
9. Odendall, C., Rolhion, N., Förster, A., Poh, J., Lamont, D. J., Liu, M., Freemont, P. S., Catling, A. D., and Holden, D. W. (2012) The *Salmonella* kinase SteC targets the MAP kinase MEK to regulate the host actin cytoskeleton. *Cell Host Microbe* **12,** 657–668
10. Unsworth, K. E., Way, M., McNiven, M., Machesky, L., and Holden, D. W. (2004) Analysis of the mechanisms of *Salmonella*-induced actin assembly during invasion of host cells and intracellular replication. *Cell. Microbiol.* **6,** 1041–1055
11. Patel, J. C., and Galán, J. E. (2005) Manipulation of the host actin cytoskeleton by *Salmonella*–all in the name of entry. *Curr. Opin. Microbiol.* **8,** 10–15
12. Tran Van Nhieu, G., Caron, E., Hall, A., and Sansonetti, P. J. (1999) IpaC induces actin polymerization and filopodia formation during *Shigella* entry into epithelial cells. *EMBO J.* **18,** 3249–3262
13. Bruno, V. M., Hannemann, S., Lara-Tejero, M., Flavell, R. A., Kleinstein, S. H., and Galán, J. E. (2009) *Salmonella typhimurium* type III secretion effectors stimulate innate immune responses in cultured epithelial cells. *PLoS Pathog.* **5,** e1000538
14. Rogers, L. D., Brown, N. F., Fang, Y., Pelech, S., and Foster, L. J. (2011) Phosphoproteomic analysis of *Salmonella*-infected cells identifies key kinase regulators and SopB-dependent host phosphorylation events. *Sci. Signal.* **4,** rs9
15. Auweter, S. D., Bhavsar, A. P., de Hoog, C. L., Li, Y., Chan, Y. A., van der Heijden, J., Lowden, M. J., Coombes, B. K., Rogers, L. D., Stoynov, N., Foster, L. J., and Finlay, B. B. (2011) Quantitative mass spectrometry catalogues *Salmonella* pathogenicity island-2 effectors and identifies their cognate host binding partners. *J. Biol. Chem.* **286,** 24023–24035
16. Rogers, L. D., Fang, Y., and Foster, L. J. (2010) An integrated global strategy for cell lysis, fractionation, enrichment, and mass spectrometric analysis of phosphorylated peptides. *Mol. Biosyst.* **6,** 822–829
17. Kyono, Y., Sugiyama, N., Imami, K., Tomita, M., and Ishihama, Y. (2008) Successive and selective release of phosphorylated peptides captured by hydroxy acid-modified metal oxide chromatography. *J. Proteome Res.* **7,** 4585–4593
18. Rappsilber, J., Mann, M., and Ishihama, Y. (2007) Protocol for micro-purification, enrichment, pre-fractionation, and storage of peptides for proteomics using StageTips. *Nat. Protoc.* **2,** 1896–1906
19. Mortensen, P., Gouw, J. W., Olsen, J. V., Ong, S. E., Rigbolt, K. T., Bunkenborg, J., Cox, J., Foster, L. J., Heck, A. J., Blagoev, B., Andersen, J. S., and Mann, M. (2010) MSQuant, an open source platform for mass spectrometry-based quantitative proteomics. *J. Proteome Res.* **9,** 393–403
20. Cox, J., and Mann, M. (2008) MaxQuant enables high peptide identification rates, individualized p.p.b.-range mass accuracies and proteome-wide protein quantification. *Nat. Biotechnol.* **26,** 1367–1372
21. Cox, J., Neuhauser, N., Michalski, A., Scheltema, R. A., Olsen, J. V., and Mann, M. (2011) Andromeda: A peptide search engine integrated into the MaxQuant environment. *J. Proteome Res.* **10,** 1794–1805
22. Olsen, J. V., Blagoev, B., Gnad, F., Macek, B., Kumar, C., Mortensen, P., and Mann, M. (2006) Global, *in vivo*, and site-specific phosphorylation dynamics in signaling networks. *Cell* **127,** 635–648
23. Huang da, W., Sherman, B. T., and Lempicki, R. A. (2009) Systematic and integrative analysis of large gene lists using DAVID bioinformatics resources. *Nat. Protoc.* **4,** 44–57
24. Schwartz, D., and Gygi, S. P. (2005) An iterative statistical approach to the identification of protein phosphorylation motifs from large-scale data sets. *Nat. Biotechnol.* **23,** 1391–1398
25. Lachmann, A., and Ma'ayan, A. (2009) KEA: Kinase enrichment analysis. *Bioinformatics* **25,** 684–686
26. Brumell, J. H., Rosenberger, C. M., Gotto, G. T., Marcus, S. L., and Finlay, B. B. (2001) SifA permits survival and replication of *Salmonella typhimurium* in murine macrophages. *Cell. Microbiol.* **3,** 75–84
27. Ong, S. E., Blagoev, B., Kratchmarova, I., Kristensen, D. B., Steen, H., Pandey, A., and Mann, M. (2002) Stable isotope labeling by amino acids in cell culture, SILAC, as a simple and accurate approach to expression proteomics. *Mol. Cell. Proteomics.* **1,** 376–386
28. Sugiyama, N., Masuda, T., Shinoda, K., Nakamura, A., Tomita, M., and Ishihama, Y. (2007) Phosphopeptide enrichment by aliphatic hydroxy acid-modified metal oxide chromatography for nano-LC-MS/MS in proteomics applications. *Mol. Cell. Proteomics* **6,** 1103–1109
29. Deiwick, J., Nikolaus, T., Erdogan, S., and Hensel, M. (1999) Environmental regulation of *Salmonella* pathogenicity island 2 gene expression. *Mol. Microbiol.* **31,** 1759–1773
30. Schroeder, N., Mota, L. J., and Méresse, S. (2011) *Salmonella*-induced tubular networks. *Trends Microbiol.* **19,** 268–277
31. Wu, R., Dephoure, N., Haas, W., Huttlin, E. L., Zhai, B., Sowa, M. E., and Gygi, S. P. (2011) Correct interpretation of comprehensive phosphorylation dynamics requires normalization by protein expression changes. *Mol. Cell. Proteomics* **10,** M111.009654
32. Lundberg, U., Vinatzer, U., Berdnik, D., von Gabain, A., and Baccarini, M. (1999) Growth phase-regulated induction of *Salmonella*-induced macrophage apoptosis correlates with transient expression of SPI-1 genes. *J. Bacteriol.* **181,** 3433–3437
33. Paesold, G., Guiney, D. G., Eckmann, L., and Kagnoff, M. F. (2002) Genes in the *Salmonella* pathogenicity island 2 and the *Salmonella* virulence plasmid are essential for *Salmonella*-induced apoptosis in intestinal epithelial cells. *Cell. Microbiol.* **4,** 771–781
34. Kim, J. M., Eckmann, L., Savidge, T. C., Lowe, D. C., Witthöft, T., and Kagnoff, M. F. (1998) Apoptosis of human intestinal epithelial cells after bacterial invasion. *J. Clin. Invest.* **102,** 1815–1823
35. Uchiya, K., Barbieri, M. A., Funato, K., Shah, A. H., Stahl, P. D., and Groisman, E. A. (1999) A *Salmonella* virulence protein that inhibits cellular trafficking. *EMBO J.* **18,** 3924–3933
36. Foster, L. J., Yeung, B., Mohtashami, M., Ross, K., Trimble, W. S., and Klip, A. (1998) Binary interactions of the SNARE proteins syntaxin-4, SNAP23, and VAMP-2 and their regulation by phosphorylation. *Biochemistry* **37,** 11089–11096
37. McGhie, E. J., Brawn, L. C., Hume, P. J., Humphreys, D., and Koronakis, V. (2009) *Salmonella* takes control: Effector-driven manipulation of the host. *Curr. Opin. Microbiol.* **12,** 117–124
38. McGhie, E. J., Hayward, R. D., and Koronakis, V. (2004) Control of actin turnover by a *Salmonella* invasion protein. *Mol. Cell* **13,** 497–510
39. Lee, S. H., and Dominguez, R. (2010) Regulation of actin cytoskeleton dynamics in cells. *Mol. Cells* **29,** 311–325
40. Rodriguez, C. I., and Stewart, C. L. (2007) Disruption of the ubiquitin ligase HERC4 causes defects in spermatozoon maturation and impaired fertility. *Dev. Biol.* **312,** 501–508
41. Cotta-Ramusino, C., McDonald, E. R., 3rd, Hurov, K., Sowa, M. E., Harper, J. W., and Elledge, S. J. (2011) A DNA damage response screen identifies RHINO, a 9-1-1 and TopBP1-interacting protein required for ATR signaling. *Science* **332,** 1313–1317
42. Saeki, K., Miura, Y., Aki, D., Kurosaki, T., and Yoshimura, A. (2003) The B cell-specific major raft protein, Raftlin, is necessary for the integrity of lipid raft and BCR signal transduction. *EMBO J.* **22,** 3015–3026
43. Keranen, L. M., Dutil, E. M., and Newton, A. C. (1995) Protein kinase C is regulated in vivo by three functionally distinct phosphorylations. *Curr. Biol.* **5,** 1394–1403
44. Mecklenbräuker, I., Saijo, K., Zheng, N. Y., Leitges, M., and Tarakhovsky, A. (2002) Protein kinase Cδ controls self-antigen-induced B-cell tolerance. *Nature* **416,** 860–865
45. LaGory, E. L., Sitailo, L. A., and Denning, M. F. (2010) The protein kinase Cδ catalytic fragment is critical for maintenance of the G_2/M DNA damage checkpoint. *J. Biol. Chem.* **285,** 1879–1887
46. Gu, Y., Rosenblatt, J., and Morgan, D. O. (1992) Cell cycle regulation of CDK2 activity by phosphorylation of Thr-160 and Tyr-15. *EMBO J.* **11,** 3995–4005
47. Li, H., Xu, H., Zhou, Y., Zhang, J., Long, C., Li, S., Chen, S., Zhou, J. M., and Shao, F. (2007) The phosphothreonine lyase activity of a bacterial type III effector family. *Science* **315,** 1000–1003
48. Haneda, T., Ishii, Y., Shimizu, H., Ohshima, K., Iida, N., Danbara, H., and Okada, N. (2012) *Salmonella* type III effector SpvC, a phosphothreonine lyase, contributes to reduction in inflammatory response during intestinal

phase of infection. *Cell. Microbiol.* **14,** 485–499
49. Navarro, L., Koller, A., Nordfelth, R., Wolf-Watz, H., Taylor, S., and Dixon, J. E. (2007) Identification of a molecular target for the *Yersinia* protein kinase A. *Mol. Cell.* **26,** 465–477
50. Rogers, L. D., Kristensen, A. R., Boyle, E. C., Robinson, D. P., Ly, R. T., Finlay, B. B., and Foster, L. J. (2008) Identification of cognate host targets and specific ubiquitylation sites on the *Salmonella* SPI-1 effector SopB/SigD. *J. Proteomics* **71,** 97–108
51. Favata, M. F., Horiuchi, K. Y., Manos, E. J., Daulerio, A. J., Stradley, D. A., Feeser, W. S., Van Dyk, D. E., Pitts, W. J., Earl, R. A., Hobbs, F., Copeland, R. A., Magolda, R. L., Scherle, P. A., and Trzaskos, J. M. (1998) Identification of a novel inhibitor of mitogen-activated protein kinase kinase. *J. Biol. Chem.* **273,** 18623–18632
52. Shinzawa, N., Nelson, B., Aonuma, H., Okado, K., Fukumoto, S., Miura, M., and Kanuka, H. (2009) p38 MAPK-dependent phagocytic encapsulation confers infection tolerance in *Drosophila*. *Cell Host Microbe* **6,** 244–252
53. Tattoli, I., Sorbara, M. T., Vuckovic, D., Ling, A., Soares, F., Carneiro, L. A., Yang, C., Emili, A., Philpott, D. J., and Girardin, S. E. (2012) Amino acid starvation induced by invasive bacterial pathogens triggers an innate host defense program. *Cell Host Microbe* **11,** 563–575
54. During, R. L., Gibson, B. G., Li, W., Bishai, E. A., Sidhu, G. S., Landry, J., and Southwick, F. S. (2007) Anthrax lethal toxin paralyzes actin-based motility by blocking Hsp27 phosphorylation. *EMBO J.* **26,** 2240–2250
55. Butt, E., Immler, D., Meyer, H. E., Kotlyarov, A., Laass, K., and Gaestel, M. (2001) Heat shock protein 27 is a substrate of cGMP-dependent protein kinase in intact human platelets: phosphorylation-induced actin polymerization caused by HSP27 mutants. *J. Biol. Chem.* **276,** 7108–7113
56. Stokoe, D., Engel, K., Campbell, D. G., Cohen, P., and Gaestel, M. (1992) Identification of MAPKAP kinase 2 as a major enzyme responsible for the phosphorylation of the small mammalian heat shock proteins. *FEBS Lett.* **313,** 307–313
57. Fernandez-Piñar, P., Alemán, A., Sondek, J., Dohlman, H. G., Molina, M., and Martín, H. (2012) The *Salmonella typhimurium* effector SteC inhibits Cdc42-mediated signaling through binding to the exchange factor Cdc24 in *Saccharomyces cerevisiae*. *Mol. Biol. Cell* **23,** 4430–4443